Diel Growth Cycle of Isolated Leaf Discs Analyzed with a Novel, High-Throughput Three-Dimensional Imaging Method Is Identical to That of Intact Leaves[1][W]

Bernhard Biskup, Hanno Scharr, Andreas Fischbach, Anika Wiese-Klinkenberg, Ulrich Schurr, and Achim Walter*

Institute of Chemistry and Dynamics of the Geosphere ICG-3 (Phytosphere), Forschungszentrum Jülich GmbH, 52425 Jülich, Germany

Dicot leaves grow with pronounced diel (24-h) cycles that are controlled by a complex network of factors. It is an open question to what extent leaf growth dynamics are controlled by long-range or by local signals. To address this question, we established a stereoscopic imaging system, GROWSCREEN 3D, which quantifies surface growth of isolated leaf discs floating on nutrient solution in wells of microtiter plates. A total of 458 leaf discs of tobacco (*Nicotiana tabacum*) were cut at different developmental stages, incubated, and analyzed for their relative growth rates. The camera system was automatically displaced across the array of leaf discs; visualization and camera displacement took about 12 s for each leaf disc, resulting in a time interval of 1.5 h for consecutive size analyses. Leaf discs showed a comparable diel leaf growth cycle as intact leaves but weaker peak growth activity. Hence, it can be concluded that the timing of leaf growth is regulated by local rather than by systemic control processes. This conclusion was supported by results from leaf discs of Arabidopsis (*Arabidopsis thaliana*) Landsberg *erecta* wild-type plants and *starch-free1* mutants. At night, utilization of transitory starch leads to increased growth of Landsberg *erecta* wild-type discs compared with *starch-free1* discs. Moreover, the decrease of leaf disc growth when exposed to different concentrations of glyphosate showed an immediate dose-dependent response. Our results demonstrate that a dynamic leaf disc growth analysis as we present it here is a promising approach to uncover the effects of internal and external cues on dicot leaf development.

Leaf growth occurs in an ever-changing environment, to which especially the growing leaves of dicot plants are exposed. While growth zones of monocot plants are protected from direct exposure to the environment by being ensheathed by older leaves, dicot leaf growth zones have to cope with temperature and light regimes that fluctuate strongly throughout 24 h (diel cycle). Dicot leaf growth is intimately connected to light quality and quantity perceived by the organ (Dale, 1988; Van Volkenburgh, 1999), and growth intensity fluctuates characteristically throughout the diel cycle. As leaf growth is an integrating behavior that is controlled by a wide range of interconnected regulatory systems, its regulation will only be understood on the basis of a combination of appropriate analysis methods and experimental approaches addressing relevant parts of the control network. Recently, an important aspect of the connection between growth, the circadian clock, and diurnally fluctuating light intensity was revealed in Arabidopsis (*Arabidopsis thaliana*) hypocotyls (Nozue et al., 2007). During the day, light inhibits growth by inactivating the growth-promoting transcription factors phytochrome-interacting factor 4 and 5. During the first half of the night, these factors are further repressed by the circadian clock, but toward dawn, this repression finally ceases, allowing an increase of growth. All factors involved in this specific regulatory chain act locally, implying that diel growth patterns controlled by this system do not depend on an intact, systemic exchange between sink and source tissue with long-range transport of phytohormones or key metabolites.

In both hypocotyls (Nozue et al., 2007) and leaves (Wiese et al., 2007) of Arabidopsis, highest relative growth rate (RGR) is reached in the early morning. This is comparable to the diel growth cycle in tobacco (*Nicotiana tabacum*; Walter and Schurr, 2000), while other species may show RGR maxima at other times of the day (Dale, 1988; Matsubara and Walter, 2006). We raise the hypothesis that the diel growth cycle of leaves of Arabidopsis and tobacco is controlled by locally acting processes that do not strongly depend on the provision of systemically distributed substances.

Leaf disc assays have been successfully used in growth measurements (Powell and Griffith, 1960; Stiles and Van Volkenburgh, 2004; Kovács et al., 2007) and in the assessment of the effects of agrochemicals (Gibon et al., 1997; Barbagallo et al., 2003) before. It has been shown that leaf discs can grow as rapidly as intact

[1] This work was supported by Forschungszentrum Jülich GmbH. B.B. acknowledges support of his Ph.D. thesis by the Heinrich-Heine University of Düsseldorf, Germany.

* Corresponding author; e-mail a.walter@fz-juelich.de.

The author responsible for distribution of materials integral to the findings presented in this article in accordance with the policy described in the Instructions for Authors (www.plantphysiol.org) is: Hanno Scharr (h.scharr@fz-juelich.de).

[W] The online version of this article contains Web-only data.
www.plantphysiol.org/cgi/doi/10.1104/pp.108.134486

leaf tissue (Dale, 1967) and that they can react strongly upon alterations of external cues (Stahlberg and Van Volkenburgh, 1999). Leaf disc assays have a number of advantages over whole plant assays. Leaf discs require little space, allowing higher numbers of replicates. Application of treatments such as nutrient solutions or phytohormones is simple, as they do not have to be taken up by the root and be transported to the leaves. Instead, leaf discs can float on solutions of active ingredients that are presented, for example, on microtiter plates (Barbagallo et al., 2003). Finally, image-based phenotyping techniques benefit from the simple shape of leaf discs, as they allow an unoccluded view of the entire area.

Yet, the use of leaf disc assays to decipher the control of leaf growth dynamics has been limited, since precise, automatic detection of leaf disc area is difficult. Automated analysis of the projected, two-dimensional (2D) area (A_{2D}), seen from a single point above the object, should be feasible with simple camera systems but has several shortcomings. The most important one is that A_{2D} depends on leaf disc inclination. Growth rates of leaf discs that are tilted (e.g. because they adhere to the wall of the vessel they reside in) or strongly curved (e.g. due to epinastic or hyponastic growth) can only be estimated with substantial errors. Moreover, when the liquid level decreases in the course of an experiment, A_{2D} decreases solely because the object distance increases. In this case, the imaging system measures the actual growth superimposed by an apparent shrinking. While the (temperature-dependent) evaporation rate across the surface of the liquid could be determined by measuring A_{2D} of nongrowing, synthetic objects, the transpiration rate of the leaf discs may differ and thus affect water loss rate.

Hence, the aim of this study was to analyze the growth of the three-dimensional (3D) surface area (A_{3D}) of leaf discs via a stereoscopic approach (called GROWSCREEN 3D; Fig. 1) to test the hypothesis that diel leaf growth cycles of the model species tobacco and Arabidopsis are controlled locally.

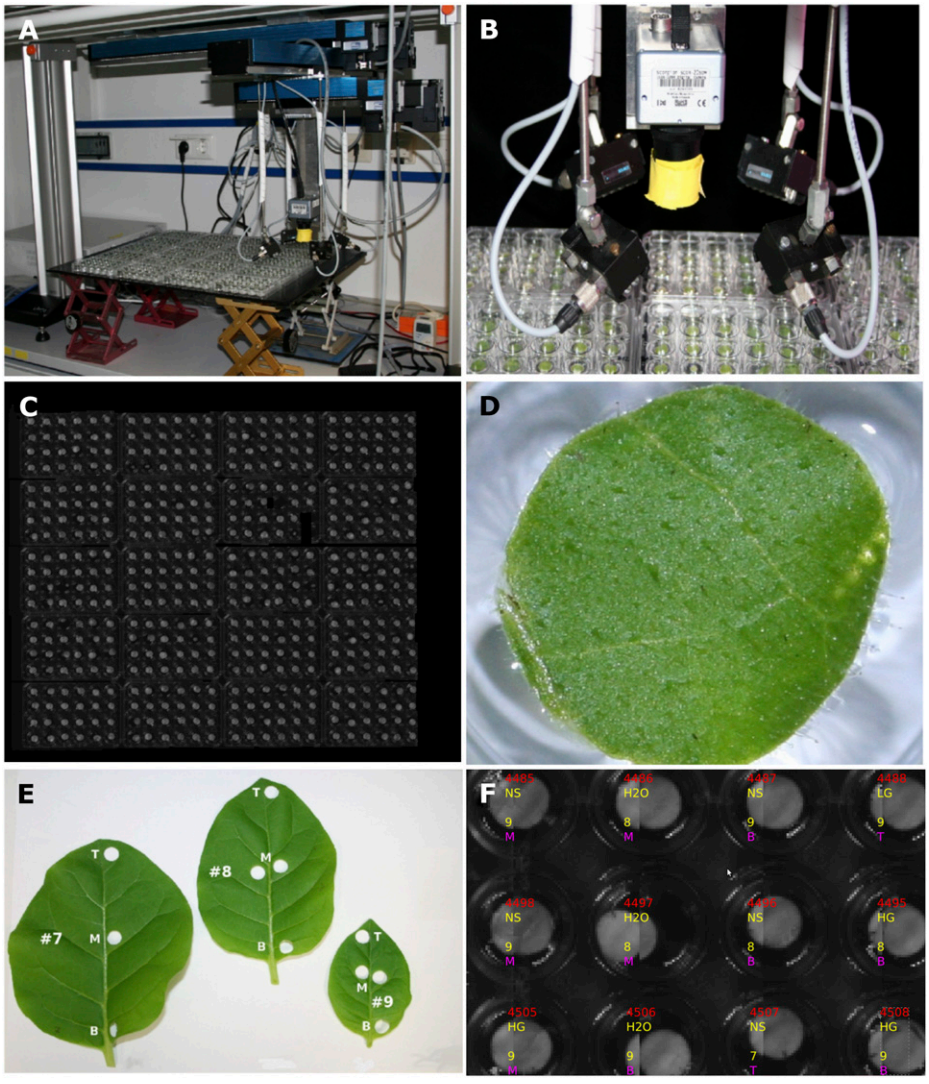

Figure 1. GROWSCREEN 3D. A, Scaffold with acquisition system. The X displacement stage is mounted to the scaffold and carries the Y and X_2 displacement stages. B, Camera surrounded by near-infrared light-emitting diode arrays. C, Overview image composed from 395 single images taken under near-infrared illumination. Some leaf discs are smaller or missing because of insufficient leaf area. D, Typical leaf disc floating in solution inside the well. The surface is slightly bent. E, Leaf numbers (counting from base, including cotyledons) and locations along the lamina (B, base; M, middle; T, tip) at which leaf discs were excised. F, Client application with superimposed information about leaf discs (plant identification number, treatment, leaf number, and location along lamina).

RESULTS

Technical Specification of the Setup

A total of 458 tobacco leaf discs, exposed to different conditions, were used for a case study of leaf growth measurements (Figs. 1 and 2). Running image acquisition at the highest possible rate, each individual leaf disc was visited approximately every 1.5 h. This corresponds to an average acquisition job duration of 11.8 s per disc, including positioning. The experiment was terminated after 72 h. With two images taken at every time point and leaf disc position, approximately 22,000 images were produced during the experiment. 3D area reconstruction was performed with very high precision by the system (Figs. 2 and 3), as described more extensively in "Materials and Methods." Further technical

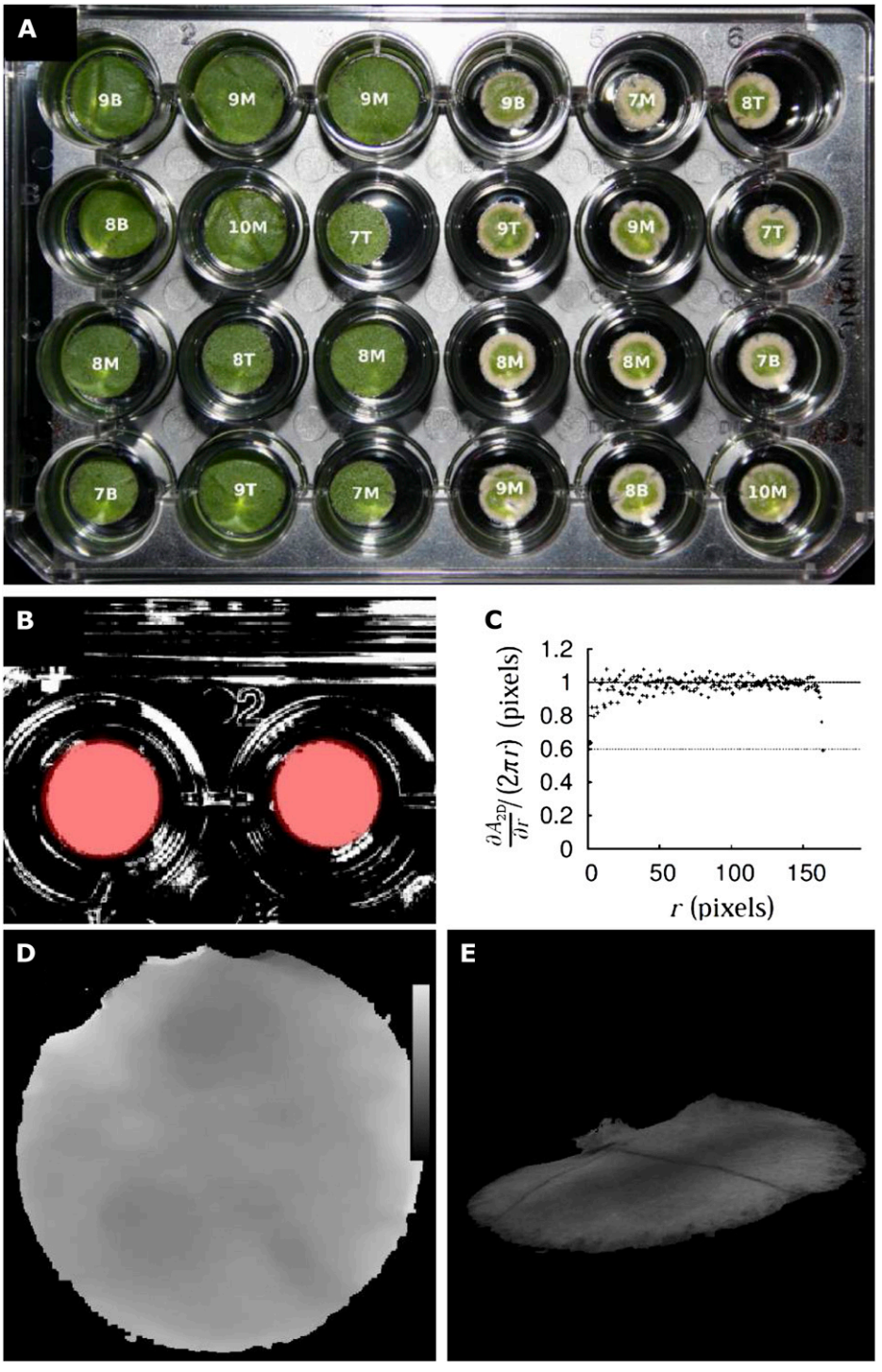

Figure 2. Examples of resulting images. A (left), Leaf discs treated with NS (nutrient solution). A (right), Leaf discs treated with HG (glyphosate at high concentration). Images were taken 72 h after the beginning of treatment. B, Binary mask M_t obtained by gray level segmentation (white, foreground; black, background); superimposed (red) are leaf disc circles as detected by computing $\partial A_{2D}/\partial r$. The final segmentation mask M_s contained those pixels of M_t closer than r to the centroid of the detected leaf disc and that had the value 1 in M_t. C, $\partial A_{2D}/\partial r$ versus r. Points show measured increase; the dashed line shows theoretical increase, $2\pi r$. D, Regularized and masked disparity map; the bar indicates the disparity range: 610 to 620 pixels. E, 3D view of a leaf disc. All depicted leaf discs are from tobacco.

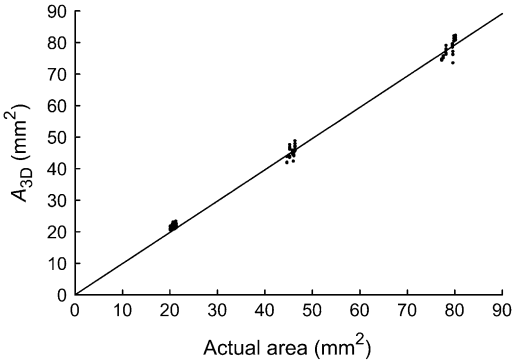

Figure 3. Accuracy of GROWSCREEN 3D determined by imaging of synthetic objects of known size. The *x* axis shows the area of paper discs determined by weighing the paper discs; the *y* axis shows A_{3D} determined using GROWSCREEN 3D. The line gives the linear fit through all data points ($y = ax$; $a = 0.991$; $R^2 = 0.9952$).

details concerning the setup and software are contained in Supplemental Appendix S1.

Base Tip Gradient and Spatial Heterogeneity of Growth

In a preliminary experiment, growth of tobacco leaf discs sampled from different leaves (leaves 7, 8, and 9) and locations along the lamina (B [base], M [middle], and T [tip]) were measured ($n = 40$) to assess the variability of growth in different regions of the plant (Walter and Schurr, 1999). This was done to determine the most suitable sampling region within the leaf canopy to test the central hypothesis on local control of leaf growth in the central experiment. Supplemental Figure S1 shows the variability of A_{3D} measured on different leaves and different locations along the lamina for the nutrient solution (NS) treatment. For locations T and B, the oldest leaves (position 7) consistently exhibited the smallest coefficients of variation [CV (A_{3D})]; younger leaves showed markedly higher CV (A_{3D}). CV (A_{3D}) in location M was similar in leaves from all positions, slowly increasing from approximately 0.025 to approximately 0.05 in the course of the experiment.

In leaves 7 and 8, a pronounced base tip gradient of growth occurred (Fig. 4). Discs cut from the base expanded more strongly than discs from the leaf tip. In leaf 9, no clear base tip gradient was found, but RGR_{3D} was higher than in leaves 7 and 8.

Since leaf 9 showed the strongest growth and since location M showed the least variability among the different leaf positions, we chose the subset of leaf discs of leaf 9, location M for detailed analysis comparing all treatments. For each replicate, A_{3D} of two subsamples (i.e. two leaf discs sampled on the same leaf; Fig. 1E) was averaged.

Growth Effects of the Incubation Solution

Leaf discs were subjected to four different treatments (Fig. 5): (1) NS; (2) water; and (3 and 4) two concentrations of the herbicide glyphosate (LG, low glyphosate; HG, high glyphosate), an inhibitor of the shikimate pathway (Steinrücken and Amrhein, 1980). The treatment effect on leaf 9, location M was tested using one-way ANOVA. Variances were homogeneous according to Levene's test ($F = 2.68$, $P = 0.06$). Treatments had a significant effect on RGR_{3D} within 24 h ($F = 93.6$, $P < 0.001$). This time interval was chosen because it integrates one full diel cycle of growth. All comparisons between treatments except for LG versus HG resulted in significant differences ($P < 0.0001$). Leaf discs from NS showed highest RGR_{3D}, whereas LG-treated leaf discs grew more slowly than leaf discs incubated in water. HG-treated leaf discs showed negative growth rates, clearly indicating senescence.

Diel Growth Cycle

NS-treated leaf discs showed characteristic diel growth variations that are clearly visible in A_{2D}, A_{3D}, and RGR_{3D} (Fig. 6). The maximum diel growth rate ($RGR_{3D,max}$) occurred at approximately 8:00 AM, reaching a peak of almost 3% h^{-1} on the first two mornings; the increase coincided with the onset of illumination. During the day, RGR_{3D} decreased, becoming even slower at 8:00 PM, when the light was switched off. On the third morning, $RGR_{3D,max}$ was only about 1.5% h^{-1}. The total increase of A_{3D} within 36 h was about 91%. In contrast, A_{2D} increased by only 81%.

The diel growth pattern was much less pronounced in water-treated leaf discs (Fig. 6F). Moreover, RGR_{3D} decayed strongly after the first 24 h, changing toward a monotonous increase superimposed by oscillations in the range of 1% h^{-1}. The 8:00 AM peak on the second morning reached only 1% h^{-1}. The total increase within 36 h was 32% for A_{3D} but only 17.4% for A_{2D}. Both glyphosate treatments caused inwardly progressing chlorosis of leaf disc borders (Fig. 2A, right), a well-known effect of glyphosate (Uotila et al., 1980; Pline-Srnic, 2005). The effect was stronger in treatment HG compared with treatment LG. Under infrared illumination, the gray values of green versus chlorotic (white) tissue did not differ; hence, area estimation was not influenced by discoloration. For LG-treated leaf discs, A_{2D} stagnated during the first hours of the experiment

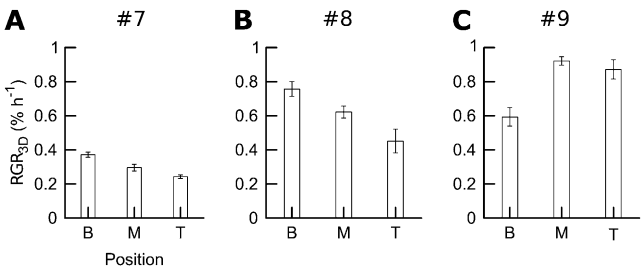

Figure 4. Base tip gradient of leaf growth in tobacco. A, Leaf 7. B, Leaf 8. C, Leaf 9. Leaf positions are as follows: B, base; M, middle; T, tip. Error bars indicate SE ($n \geq 6$). RGR_{3D} was computed between $t_1 = 0$ h and $t_2 = 48$ h.

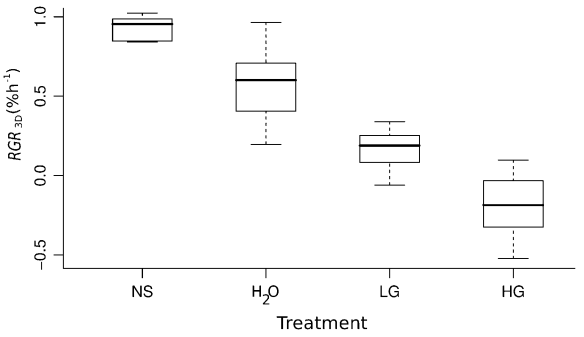

Figure 5. RGR_{3D} of leaf 9. The box plot shows the RGR_{3D} of leaf 9 between 0 h and 24 h after the beginning of the experiment, grouped by treatment ($n \geq 10$). Treatments are as follows: NS, nutrient solution; H_2O, tap water (control); LG and HG, glyphosate at low and high concentration, respectively.

and then decreased (Fig. 6G), whereas A_{3D} increased for the first hours and stagnated thereafter (Fig. 6H). Accordingly, the net change of A_{2D} over 36 h was −9.2%, while A_{3D} increased by 5.1%. $RGR_{3D,max}$ on the first morning was only 0.8% h^{-1}. Later on, oscillations of RGR_{3D} were much weaker compared with other treatments. Leaf discs of both glyphosate treatments did not grow any more at the end of the experiment. HG-treated leaf discs showed a net decrease of A_{2D} as well as A_{3D}. A_{2D} decreased almost linearly over 36 h, resulting in a net loss of 12.9%. A_{3D} first increased by about 2% and finally decreased by 3.3% with respect to the initial area. Although there was a weak RGR_{3D} peak in the morning (0.3% h^{-1}), RGR_{3D} was very low from the beginning on.

Growth of Leaf Discs of Arabidopsis (Landsberg *erecta* versus *starch-free1*)

By analogy with the tobacco experiment, leaf discs were taken from different leaves of Arabidopsis. Discs from leaf 12 showed little growth variation and were thus chosen to determine the diel growth cycle in terms of RGR_{3D} (Fig. 7). As in tobacco, Arabidopsis leaf discs of both lines (Landsberg *erecta* [L*er*] and *starch-free1* [*stf1*]) exhibited a growth maximum in the morning. The minimum growth rate occurred approximately 3 h after the light was switched off. During most of the night and in the early morning, RGR_{3D} was substantially higher in L*er* than in *stf1*. In contrast, during the second half of the day, RGR_{3D} of *stf1* plants was higher than RGR_{3D} of L*er*. The onset of RGR_{3D} increase in the morning was delayed in *stf1* in comparison with L*er*. During the night, RGR_{3D} of L*er* increased to more than 1% h^{-1}, whereas RGR_{3D} of *stf1* remained around 0.5% h^{-1}. RGR_{3D} amplitudes decayed over the observed time period. This effect was more pronounced in L*er*, for which $RGR_{3D,max}$ on the second morning was only 63% of RGR_{max} on the first morning. In contrast, $RGR_{3D,max}$ of the *stf1* mutant only decreased to 87% compared with the value obtained on the first morning.

Growth of Leaves on Intact Plants of Arabidopsis and Tobacco

For intact plants of Arabidopsis and tobacco, similar diel cycles of leaf growth activity as reported in the literature before were observed in the conditions of this study (Fig. 8). Peak values of RGR were obtained early in the morning, and RGR decreased almost to zero during the night. Peak values were higher in intact leaves compared with leaf discs. Growth phasing in Arabidopsis L*er* and *stf1* differed in the same way as described above for the leaf discs: *stf1* grew more slowly than L*er* during the night and in the first half of the day, but it was able to catch up during the second half of the day.

DISCUSSION

Performance and Possible Improvements of GROWSCREEN 3D

The performance of the distributed computer system is sufficient for high-throughput screening. Computation of RGR_{3D} time series while an experiment is running (''real-time'' evaluation) saves time by providing quick feedback. Depending on the hypothesis to be tested, data can be integrated in different ways (e.g. allowing one to investigate even higher numbers of leaf discs with a smaller temporal resolution or vice versa).

In future analyses, the determination of A_{3D} would benefit from improved image segmentation. This could be achieved by (1) more homogeneous illumination, (2) backlight illumination, which would provide better contrast because of vascular tissue, and (3) using a more refined segmentation algorithm (e.g. using a contour model; Kass et al., 1987; Osher and Sethian, 1988). An automated plate positioning system (e.g. a conveyor belt) could increase throughput, especially for scenarios in which only a few stereo images per leaf disc and per day are needed. Acquisition time per leaf disc could be decreased by using two or more cameras simultaneously. Depending on the optical system and working distance, these cameras might need to be mounted convergently to obtain sufficiently overlapping fields of view. Possible limitations of input/output rates could be alleviated by using multiple file servers and by balancing job result directories over these, possibly via separate network connections.

Diel Growth Cycle and Base Tip Gradient in Tobacco

Timing of the diel distribution of growth activity coincides well with the diurnal growth cycle of intact tobacco leaves (Walter and Schurr, 2000). This indicates clearly that the timing of the diel growth cycle is controlled by local regulatory mechanisms, such as the interplay between the phytochrome system and the circadian clock (Nozue et al., 2007) or light-induced elicitation of ion fluxes and alteration of membrane potential (Van Volkenburgh, 1999) rather than by long-

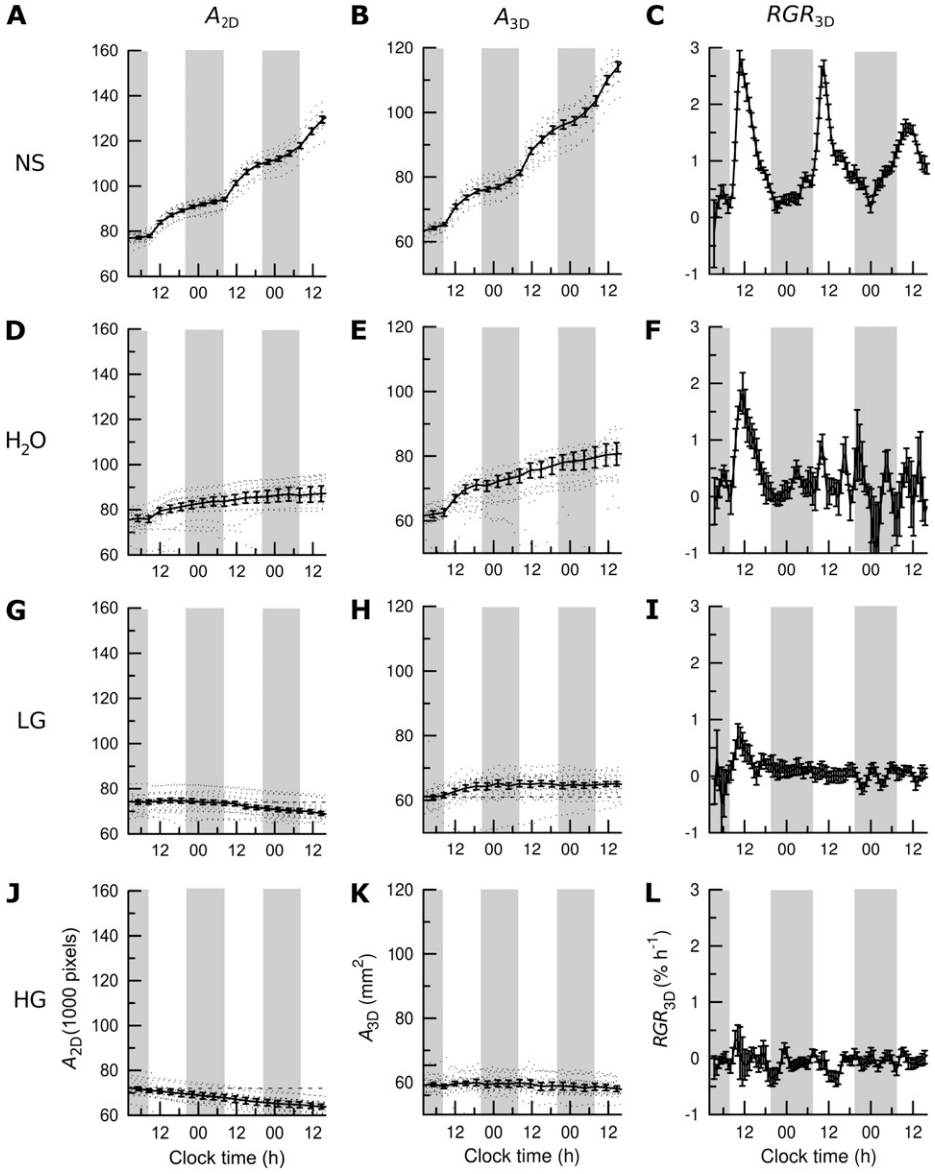

Figure 6. Time course of leaf disc area development of tobacco in A_{2D} (left panels), A_{3D} (middle panels), and RGR_{3D} (right panels). Time courses were measured on leaf 9, middle location. A to C, Treatment NS (nutrient solution). D to F, Treatment H_2O (tap water control). G to I, Treatment LG (low glyphosate concentration). J to L, Treatment HG (high glyphosate concentration). Dot traces indicate time course of areas of individual leaf discs. Solid curves show median ± SE (HG, $n = 9$; LG, $n = 9$; NS, $n = 8$; H_2O, $n = 9$). Dotted curves show A_{3D} of individual leaf discs (including outliers). Dashed horizontal lines in LG and HG indicate areas at the beginning of measurement to illustrate the net effect of superimposed growth and the perceived shrinking due to decreasing water level. RGR_{3D} was calculated from the time course of A_{3D} (mean ± SE). Shaded vertical bars in the background of each panel indicate night.

distance signaling via import of hormones (Rahayu et al., 2005) or carbohydrates from source leaves. The necessity of an intact local metabolism for undisturbed diel growth performance is demonstrated by the vanishing diel growth cycle in leaf discs treated with glyphosate (Fig. 5, I and L). Glyphosate is known to primarily inhibit the shikimate pathway (Steinrücken and Amrhein, 1980) and subsequently affects general metabolic processes, such as protein synthesis, photosynthesis, and carbon metabolism (Geiger et al., 1986, 1987; de María et al., 2005). Lower peak growth rates of leaf discs compared with leaves from intact plants (compare Figs. 6, 7, and 8) might be caused by missing carbohydrate import from source tissue. Although it is known from short-term experiments with excised leaf tissue that intact photosynthesis is not a prerequisite for short-term growth reactions (Dale, 1988; Van Volkenburgh, 1999), a coordinated supply with carbohydrates for cell wall assembly and other purposes, from storage pools, source tissue, or local photosynthesis, is essential to sustain the timing of diel growth cycles for days. In addition to an undisturbed timing of carbohydrate availability, sufficient external supply of mineral nutrients is required for coordinated diel growth activity lasting several days in isolated leaf discs (Figs. 5 and 6C).

The base tip gradient in leaves 7 and 8 (Fig. 4, A and B) is in accordance with the relations in intact, growing leaves and results from the delayed initiation of the tissue at leaf emergence (Walter and Schurr, 1999). Cell expansion rate reduces with age, which is reflected by the highest RGR at the base and the lowest RGR at the tip, where cell expansion has proceeded for a longer time. In the developmental stage, at which samples were taken from leaves 7 and 8, cell divisions have

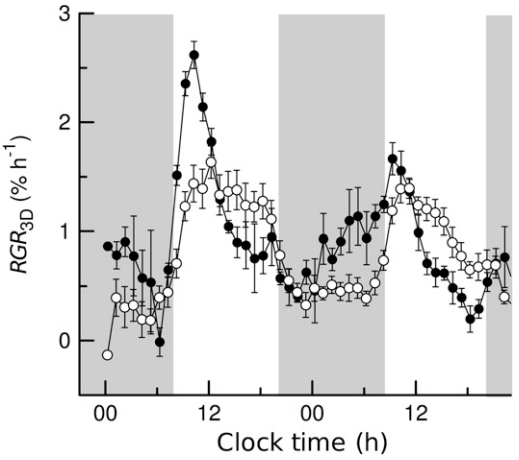

Figure 7. Diel growth cycles of leaf discs of two genotypes of Arabidopsis. Leaf discs of L*er* (black circles) and *stf1* (white circles) were grown in NS. Individual area measurements were smoothed using a 2.5-h running average filter. Shaded vertical bars in the background indicate night. RGR_{3D} values are given ±SE ($n \geq 3$).

ceased at both the leaf tip and the base (Walter et al., 2003). The reversed base tip gradient in leaf 9 (Fig. 4C) might be due to cell division activity that can still be found in the leaf base of this developmental stage and with the slower rate of cell expansion in dividing cells. For undisturbed expansion of this tissue, long-distance signals might still be crucial.

For two reasons, the quality of the results increases markedly when 3D information (A_{3D}) instead of 2D information (A_{2D}) is used (Fig. 6). The first reason is that evaporation and transpiration cause the water level to decrease during a screening experiment. Using A_{3D} instead of A_{2D} allows compensating for the perceived area decrease in perspective projection. This effect may be negligible in the presence of pronounced positive RGR (e.g. under NS treatment); however, to correctly measure weaker growth rates, the compensation is clearly necessary, as it may even cause a sign reversal of RGR (apparent shrinking of leaf discs; e.g. HG treatment; Fig. 6J). The second reason is the distortion of the leaf discs during the experiment (Fig. 2): most leaf discs develop from flat discs into buckling ovate sheets, making it necessary to follow the topography of the object in three dimensions to capture its surface area correctly.

Altered Diel Growth Cycle of an Arabidopsis Mutant

Diel growth cycles of the L*er* wild type and the *stf1* mutant of Arabidopsis were measured using GROWSCREEN 3D. The observed patterns are in good agreement with previous observations by Wiese et al. (2007). There, the growth cycles of the two lines were characterized in leaves of intact plants by means of a well-established, noninvasive digital image sequence processing (DISP) technique, along with measurements of diel carbohydrate metabolism. Yet, the DISP technique has two major shortcomings. On the one hand, leaves need to be mechanically constrained in the focal plane of the camera, as nyctinastic movements of the entire plant would make quantitative analyses impossible. On the other hand, only small replicate numbers are possible with this technique, as one camera can only visualize the growth of one leaf. The different growth kinematics of L*er* and *stf1* can be explained by the way that the *stf1* mutation affects the diel carbohydrate availability (Kofler et al., 2000). In the daytime, the inability to synthesize starch causes an excess of hexoses to be available; thus, higher RGR in comparison with L*er* can be maintained by *stf1* mutants. In contrast, in the nighttime, the lack of mobilizable starch reduces *stf1* RGR. This explains the overall weaker growth in *stf1*, which has been observed by other authors for starch-free mutants before (Caspar et al., 1985; Huber and Hanson, 1992). The similarities between DISP and GROWSCREEN 3D analyses are striking, given that the growth phenotypes were observed in completely different systems (leaf discs versus intact plants). The difference between L*er* and *stf1* indicates clearly that even transitory starch produced in the growing leaf, and not in fully developed source leaves, is sufficient to drive the coordinated growth activity of the leaf tissue. Again, this underlines the

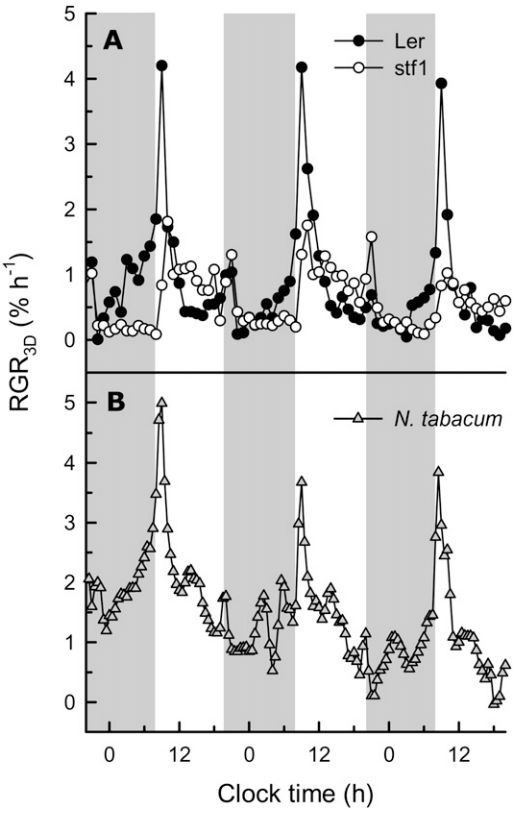

Figure 8. Leaf growth dynamics of individual intact leaves as determined by the DISP method. A, Arabidopsis. B, Tobacco. Shaded vertical bars in the background indicate night.

importance of local regulatory mechanisms controlling the diel expansion of leaf tissue.

CONCLUSION

This study introduced an image-based phenotyping system for leaf discs that uses 3D information to compensate for tissue surface deformations and sinking water levels, overcoming major disadvantages of leaf discs for growth analyses. The system has the potential for high-throughput growth assays and is capable of resolving detrimental and beneficial effects of substances added to the incubation solution. Due to the high precision of the system, characteristic features of the diel growth activity of Arabidopsis and tobacco leaf discs were obtained. Diel growth cycles of leaf discs resembled those of intact leaves attached to the plant very closely, demonstrating the importance of local control mechanisms on the timing of dicot leaf expansion.

MATERIALS AND METHODS

Imaging System of GROWSCREEN 3D

A brief description of the system and image-processing procedures is given below; for a more detailed description of the hardware and software (including sources of supply), refer to the Supplemental Appendix S1. GROWSCREEN 3D (Fig. 1) is based on the mechanical design of the 2D screening setup GROWSCREEN (Walter et al., 2007). Two moving stages (Fig. 1A; X and Y) are used to move a 2-megapixel camera in the horizontal plane. A third moving stage (X_2) facilitates horizontal displacement for acquiring stereo image pairs. The camera is directed downward and equipped with an infrared long-pass filter. The scene is illuminated by four near-infrared light-emitting diode arrays (Fig. 1B; wavelength, 880 nm), because near-infrared illumination is physiologically inactive. Leaf discs under investigation are kept on 24-well Microtiter plates (Fig. 5A; well volume, 2.5 mL). Lids are removed for the duration of the experiment to ensure gas exchange and to avoid fogging, which would hamper imaging. At each camera position (X and Y), two images are taken, using a stereo baseline (displacement of moving stage X_2) of b = 20 mm.

Image Segmentation

The purpose of image segmentation is to separate leaf discs from background. A clean segmentation is a prerequisite to precise area measurements. Because images are acquired in near-infrared light, only grayscale images are available. This allows image acquisition throughout day and night but makes segmentation more challenging in comparison with color images (Russ, 2002; Walter et al., 2007). Therefore, the following segmentation procedure is applied (Fig. 2). (1) Images are corrected for illumination uniformity. (2) Gray level thresholding is applied to remove most of the background. (3) Morphological erosion is applied to clean up the segmentation mask. (4) Leaf disc borders are detected. (5) Candidate leaf discs from both images of a pair are matched. (6) For a newly detected leaf disc, a unique identification number is assigned. (7) The projected area A_{2D} is computed for each leaf disc.

Stereo Matching and 3D Reconstruction

To measure A_{3D} and ultimately RGR_{3D}, surface models at different time points are required. Using leaf discs detected by image segmentation, 3D surface models are obtained as follows. (1) Image distortions are removed and images are rectified such that corresponding features share the same y coordinate in both images of a pair. (2) A stereo matching algorithm (Faugeras et al., 1993) is applied to compute a disparity map (a map of displacements; Fig. 2D). (3) Outliers are removed. (4) 3D coordinates are recovered by stereo triangulation. (5) The surface model is smoothed. (6) The leaf disc surface area A_{3D} is computed (Fig. 2E).

Setup Calibration

Measurement accuracy is affected by a multitude of parameters: quality of camera and stereo calibration, position of an object in the images, object shape, object distance, object inclination, object size, color, texture, reflections, and stereo baseline, to name only some. We chose to limit our accuracy considerations to the following parameters that are most relevant to the presented study: leaf disc size (varying because of growth), object distance (varying because of sinking water level), curvature (varying because of increased bending of leaf discs during the experiment), and inclination, which changes, for example, when floating leaf discs begin to adhere to the vessel wall.

For each of these four parameters, two to three values spanning the range of expected values were selected and several replicate calibration targets were produced. This resulted in a total number of 96 calibration measurements. As calibration targets, circular paper discs with nominal diameters of 5, 7.5, and 10 mm and with leaf-like texture were printed on laser printer paper (80 g m^{-2}) and cut out. In order to determine their actual area, the discs were weighed using a laboratory scale (accuracy, 0.01 mg). Eight paper discs of each nominal diameter were glued to the round wall of a black, horizontal cylinder (diameter, 16.5 mm). Half of the discs of one diameter touched the cylinder along their entire surface, thus having the same curvature as the cylinder. The other half were connected to the cylinder only in the middle and were therefore planar. The planar discs were mounted exactly on top of the cylinder. The curved discs were mounted off-center, covering an inclination range from $-36°$ to $+36°$ around the center. Synthetic leaf discs were imaged at distances of 107, 112, 117, and 122 mm from the image plane, covering the object distances realized in the experiments.

Figure 3 shows the depiction of A_{3D} versus the area determined by weighing the paper discs. For the other three parameters tested in this calibration procedure (disc curvature, distance, and inclination), no systematic effect on A_{3D} was determined; each calibration measurement is included as a data point in Figure 3. The slight deviation of the inclination of the fit line from unity results from the weight of the laser toner printed on the calibration targets. The results demonstrate that the accuracy of GROWSCREEN 3D is sufficient for measuring leaf disc areas and consequently RGR of leaf discs in ranges encountered in typical measurement configurations. It should be noted that RGR computation does not even require absolute area measurements, because only area ratios are used.

DISP Leaf Growth Analysis in Intact Plants

Leaves were mechanically constrained to the focal plane of a camera and analyzed for RGR by a procedure described in more detail elsewhere (Walter and Schurr, 2000; Wiese et al., 2007). In short, images of flat leaves were illuminated in the near-infrared wavelength range (880 nm), ensuring image acquisition at constant brightness throughout day and night. Structural elements of the leaves, such as trichomes and vein intersections, are followed throughout parts of an image sequence, and the divergence of structural elements with time renders the relative growth rate of the tissue between structural elements. Plants were exposed to the same environmental conditions as for the leaf disc experiments.

Plant Material and Cultivation Procedures

Seeds of tobacco (*Nicotiana tabacum* 'Samsun') were germinated on well-watered soil ED73 (Einheitserde, Balster Einheitserdewerk; approximately 250 mg L^{-1} nitrogen, approximately 300 mg L^{-1} P_2O_5, and approximately 400 mg L^{-1} K_2O). Prior to experiments, plants were cultivated in a greenhouse in winter with a photoperiod of 12 h/12 h of light/dark. Plants were acclimated to laboratory conditions (50 μmol m^{-2} s^{-1} photosynthetically active radiation; same photoperiod; peak day temperature, 24.9°C; night temperature, 22.9°C; oscillations due to change in illumination) 24 h before the experiment began. Plants were 31 d old and vegetative at the beginning of the experiment.

Leaf discs were excised using a cork borer (9 mm i.d.) from defined locations along the lamina at the base (B), middle (M), and tip (T) of still expanding leaves 7, 8, and 9 (counting from bottom to top, including cotyledons; Fig. 1, D and E). Leaf discs were immediately transferred to their respective treatment solution, floating adaxial (top) side up.

Arabidopsis (*Arabidopsis thaliana*) plants were grown in soil in a growth chamber (125 μmol m^{-2} s^{-1} photosynthetically active radiation with a 12-h/12-h light/dark period; temperature, 23°C during the day, 18°C at night; relative humidity, 60% during the day, 65% at night). The starch-free mutant *stf1* (Kofler et al., 2000) carries a 55-bp deletion in the plastidic phosphoglucomutase gene in the background of the L*er* ecotype. Seeds for *stf1* were obtained from Dr. H. Kofler (University of Cologne). Arabidopsis plants were 32 d old and vegetative at the beginning of the experiment.

Leaf discs were excised using a cork borer (5 mm i.d.) from the middle of leaf 12, excluding the midvein.

Treatments

Tobacco leaf discs were subjected to four different treatments: (1) NS (1:10 Hakaphos nutrient solution; Hakaphos Blau) full-strength solution was prepared according to the manufacturer's specification for young flowering plants and contained 15% (w/w) nitrogen, 10% (w/w) P_2O_5, 15% (w/w) K_2O, 2% (w/w) MgO, 0.01% (w/w) boron, 0.02% (w/w) copper, 0.05% (w/w) iron, 0.05% (w/w) manganese, 0.001% (w/w) molybdenum, and 0.015% (w/w) zinc (Ca^{2+} and SO_4^{2-} were contained in tap water); (2) tap water; (3) LG, low concentration of glyphosate (0.74 μmol L^{-1}; *N*-(phosphonomethyl)Gly; Clinic Nufarm); (4) HG, high concentration of glyphosate (74 μmol L^{-1}). Treatments were applied on 24-well Microtiter plates in 2 mL of liquid volume per leaf disc. The typical time until total evaporation was approximately 7 d. Leaf discs of both Arabidopsis lines were only subjected to treatment NS (see above).

Due to evaporation and water/nutrient uptake by the growing leaf disc, nutrient concentrations can decrease or increase during the experiment, depending on RGR and evaporative demand. pH of the nutrient solution is buffered to values between 5 and 6, depending on the strength of the solution.

Growth Rates

Assuming exponential growth of the form $A(t_2) = A(t_1)\, e^{RGR(t_2 - t_1)}$, RGRs of leaf tissue are determined as

$$RGR[\%/\mathrm{d}] = \frac{100}{t_2 - t_1} \ln \frac{A(t_2)}{A(t_1)}$$

where $A(t_2)$ and $A(t_1)$ are projected or actual 3D areas at two time points, t_1 and t_2 (Walter and Schurr, 1999).

Statistics

All statistical computations were carried out using the R statistics package (R Foundation). A_{3D} values more distant from the group median than ± 2 SDS were considered outliers and discarded. Treatments were compared using one-way ANOVA (Faraway, 2005). Homogeneity of variances was tested using Levene's test (Levene, 1960). Pairwise comparisons of treatments were done with a pairwise *t* test, adjusting *P* values using Holm's correction (Holm, 1979).

Supplemental Data

The following materials are available in the online version of this article.

Supplemental Figure S1. Variability of area measurements.

Supplemental Figure S2. Deployment of the GROWSCREEN 3D system.

Supplemental Figure S3. Database scheme.

Supplemental Figure S4. Activity diagram of essential workflow steps.

Supplemental Figure S5. Scalability of job execution.

Supplemental Table S1. Most important database tables.

Supplemental Table S2. Third-party software.

Supplemental Table S3. Artificial job types for scalability measurements.

Supplemental Appendix S1. Technical details of GROWSCREEN 3D.

ACKNOWLEDGMENTS

We are grateful to S. Briem and G. Dreissen, who developed parts of the client software of our screening system; to A. Averesch, who maintained the network infrastructure; and to B. Uhlig for plant cultivation. M.M. Christ kindly conducted preliminary experiments on leaf discs, and H. Kofler provided seeds of the Arabidopsis *stf1* mutant.

Received December 17, 2008; accepted January 12, 2009; published January 23, 2009.

LITERATURE CITED

Barbagallo RP, Oxborough K, Pallett KE, Baker NR (2003) Rapid, noninvasive screening for perturbations of metabolism and plant growth using chlorophyll fluorescence imaging. Plant Physiol **132:** 483–493

Caspar T, Huber SC, Somerville C (1985) Alterations in growth, photosynthesis, and respiration in a starchless mutant of *Arabidopsis thaliana* (L.) deficient in chloroplast phosphoglucomutase activity. Plant Physiol **79:** 11–17

Dale JE (1967) Growth changes in disks cut from young leaves of Phaseolus. J Exp Bot **18:** 660–671

Dale JE (1988) The control of leaf expansion. Annu Rev Plant Physiol Plant Mol Biol **39:** 267–295

de María N, de Felipe MR, Fernández-Pascual M (2005) Alterations induced by glyphosate on lupin photosynthetic apparatus and nodule ultrastructure and some oxygen diffusion related proteins. Plant Physiol Biochem **43:** 985–996

Faraway JJ (2005) Linear Models with R. Texts in Statistical Science, Vol 63. CRC Press, Boca Raton, FL, pp 179–186

Faugeras O, Hotz B, Mathieu H, Viéville T, Zhang Z, Fua P, Théron E, Moll L, Berry G, Vuillemin J, et al (1993) Real Time Correlation Based Stereo: Algorithm Implementations and Applications. Technical Report 2013. INRIA Sophia Antipolis, Sophia Antipolis, France, pp 4–12

Geiger DR, Kapitan SW, Tucci M (1986) Glyphosate inhibits photosynthesis and allocation of carbon to starch in sugar beet leaves. Plant Physiol **82:** 468–472

Geiger DR, Tucci MA, Serviates JC (1987) Glyphosate effects on carbon assimilation and gas exchange in sugar beet leaves. Plant Physiol **85:** 365–369

Gibon Y, Bessières MA, Larher F (1997) Is glycine betaine a non-compatible solute in higher plants that do not accumulate it? Plant Cell Environ **20:** 329–340

Holm S (1979) A simple sequentially rejective multiple test procedure. Scand J Stat **6:** 65–70

Huber SC, Hanson KR (1992) Carbon partitioning and growth of a starchless mutant of *Nicotiana sylvestris*. Plant Physiol **99:** 1449–1454

Kass M, Witkin A, Terzopoulos D (1987) Snakes: active contour models. Int J Comput Vis **1:** 321–331

Kofler H, Häusler RE, Schulz B, Gröner F, Flügge UI, Weber A (2000) Molecular characterisation of a new mutant allele of the plastid phosphoglucomutase in *Arabidopsis*, and complementation of the mutant with the wild-type cDNA. Mol Gen Genet **263:** 978–986

Kovács E, Sárvári E, Nyitrai P, Darók J, Cseh E, Láng F, Keresztes A (2007) Structural-functional changes in detached cucumber leaves, and modelling these by hormone-treated leaf discs. Plant Biol **9:** 85–92

Levene H (1960) Robust tests for equality of variances. *In* Contributions to Probability and Statistics. Stanford University Press, Stanford, CA, pp 278–292

Matsubara S, Walter A (2006) Living in day-night cycles: specific diel leaf growth patterns and the circadian control of photomorphogenesis. Prog Bot **68:** 288–314

Nozue K, Covington MF, Duek PD, Lorrain S, Fankhauser C, Harmer SL, Maloof JN (2007) Rhythmic growth explained by coincidence between internal and external cues. Nature **448:** 358–363

Osher S, Sethian JA (1988) Fronts propagating with curvature dependent speed: algorithms based on Hamilton-Jacobi formulation. J Comput Phys **79:** 12–49

Pline-Srnic W (2005) Technical performance of some commercial glyphosate-resistant crops. Pest Manag Sci **61:** 225–234

Powell R, Griffith M (1960) Some anatomical effects of kinetin and red light on disks of bean leaves. Plant Physiol **35:** 273–275

Rahayu YS, Walch-Liu P, Neumann G, Römheld V, von Wiren N, Bangerth F (2005) Root-derived cytokinins as long-distance signals for NO_3-induced stimulation of leaf growth. J Exp Bot **56:** 1143–1152

Russ JC (2002) The Image Processing Handbook, Ed 5. CRC Press, Boca Raton, FL, pp 408–412

Stahlberg R, Van Volkenburgh E (1999) The effect of light on membrane potential, apoplastic pH and cell expansion in leaves of *Pisum sativum* L. var. Argenteum. Planta **208:** 188–195

Steinrücken HC, Amrhein N (1980) The herbicide glyphosate is a potent inhibitor of 5-enol pyruvyl-shikimic acid-3-phosphate synthase. Biochem Biophys Res Commun **94:** 1207–1212

Stiles KA, Van Volkenburgh E (2004) Role of K^+ in leaf growth: K^+ uptake is required for light-stimulated H^+ efflux but not solute accumulation. Plant Cell Environ **27:** 315–325

Uotila M, Evjen K, Iversen TH (1980) The effects of glyphosate on the development and cell infrastructure of white mustard (*Sinapis alba* L.) seedlings. Weed Res **20:** 153–158

Van Volkenburgh E (1999) Leaf expansion: an integrating plant behaviour. Plant Cell Environ **22:** 1463–1473

Walter A, Roggatz U, Schurr U (2003) Expansion kinematics are an intrinsic property of leaf development and are scaled from cell to leaf level at different nutrient availability. Plant Biol **5:** 642–650

Walter A, Scharr H, Gilmer F, Zierer R, Nagel KA, Ernst M, Wiese A, Virnich O, Christ MM, Uhlig B, et al (2007) Dynamics of seedling growth acclimation towards altered light conditions can be quantified via GROWSCREEN: a setup and procedure designed for rapid optical phenotyping of different plant species. New Phytol **174:** 447–455

Walter A, Schurr U (1999) The modular character of growth in *Nicotiana tabacum* plants under steady-state nutrition. J Exp Bot **50:** 1169–1177

Walter A, Schurr U (2000) Spatio-temporal variation of leaf growth, development and function. *In* B Marshall, J Roberts, eds, Leaf Development and Canopy Growth. Sheffield Academic Press, Sheffield, UK, pp 96–118

Wiese A, Christ MM, Virnich O, Schurr U, Walter A (2007) Spatio-temporal leaf growth patterns of *Arabidopsis thaliana* and evidence for sugar control of the diel leaf growth cycle. New Phytol **174:** 752–761